Cell PRESS
Open ACCESS

Cell Reports
Report

Removal of Polycomb Repressive Complex 2 Makes *C. elegans* Germ Cells Susceptible to Direct Conversion into Specific Somatic Cell Types

Tulsi Patel,[1,2] Baris Tursun,[1,2,3] Dylan P. Rahe,[1] and Oliver Hobert[1,*]
[1]Department of Biochemistry and Molecular Biophysics, Howard Hughes Medical Institute, Columbia University Medical Center, New York, NY 10032, USA
[2]These authors contributed equally to this work
[3]Present address: Berlin Institute for Medical Systems Biology, Max Delbrück Center for Molecular Medicine, Berlin 13125, Germany
*Correspondence: or38@columbia.edu
http://dx.doi.org/10.1016/j.celrep.2012.09.020

SUMMARY

How specific cell types can be directly converted into other distinct cell types is a matter of intense investigation with wide-ranging basic and biomedical implications. Here, we show that removal of the histone 3 lysine 27 (H3K27) methyltransferase Polycomb repressor complex 2 (PRC2) permits ectopically expressed, neuron-type-specific transcription factors ("terminal selectors") to convert *Caenorhabditis elegans* germ cells directly into specific neuron types. Terminal-selector-induced germ-cell-to-neuron conversion can be observed not only upon genome-wide loss of H3K27 methylation in PRC2(−) animals but also upon genome-wide redistribution of H3K27 methylation patterns in animals that lack the H3K36 methyltransferase MES-4. Manipulation of the H3K27 methylation status not only permits conversion of germ cells into neurons but also permits *hlh-1/MyoD*-dependent conversion of germ cells into muscle cells, indicating that PRC2 protects the germline from the aberrant execution of multiple distinct somatic differentiation programs. Taken together, our findings demonstrate that the normally multistep process of development from a germ cell via a zygote to a terminally differentiated somatic cell type can be short-cut by providing an appropriate terminal selector transcription factor and manipulating histone methylation patterns.

INTRODUCTION

A number of transcription factors are known to be absolutely required for the induction of specific cellular differentiation programs. However, such transcription factors are often remarkably inefficient at imposing such a program on other cell types upon ectopic misexpression (Zhou and Melton, 2008). For example, ectopic misexpression of the CHE-1 zinc finger transcription factor, which is normally required to generate the ASE gustatory neuron type in *Caenorhabditis elegans* (Chang et al., 2003; Uchida et al., 2003), converts only a very small number of sensory neurons into ASE-like neurons; all other cell types are immune to the cell-fate-inducing ability of *che-1* (Tursun et al., 2011).

To explore the context dependency of *che-1* activity, we considered the possibility that an inhibitory mechanism may exist to prevent *che-1* from driving the ASE differentiation program in most other cell types. With this possibility in mind, we undertook a loss-of-function screen for genes whose knockdown enables *che-1* to more broadly induce ASE-like fate in other cellular contexts. This RNA interference (RNAi)-based screen identified a phylogenetically conserved histone chaperone, *lin-53* (called Rbbp4 and Rbbp7 in vertebrates), whose removal permitted a direct, *che-1*-mediated conversion of mitotic germ cells into ASE-like neurons (Tursun et al., 2011).

In this work, we explored the mechanistic basis of the conversion process by asking which other genes are involved in this process. We based our analysis on the well-documented observations that in vertebrates and invertebrates, the histone chaperones LIN-53/Rbbp4,7 are components of many distinct multiprotein complexes with various functions in chromatin biology. These complexes include the nucleosome remodeling and histone deacetylation (NURD) complex, the chromatin assembly factor (CAF) complex, the histone deacetylase corepressor complex Sin3, the histone acetyltransferase 1 (HAT1) complex, the nucleosome remodeling factor (NURF) complex, the retinoblastoma-gene-containing repressor complex DP, Rb, and class B synMuv (DRM), and Polycomb repressive complex 2 (PRC2) (Harrison et al., 2006; Loyola and Almouzni, 2004). The presence of LIN-53/Rbbp4,7 in these functionally very distinct complexes has been shown biochemically as well as through genetic analysis. Here, we show that the effect of *lin-53* on germ-cell-to-neuron conversion can be phenocopied by removal of the PRC2 complex, and further characterize features of the cellular conversion process.

RESULTS AND DISCUSSION

Removal of PRC2 Complex Components Allows for Germ-Cell-to-Neuron Conversion

Our initial RNAi screen, which showed that *lin-53* functions as a brake against the conversion of germ cells to neurons (Tursun

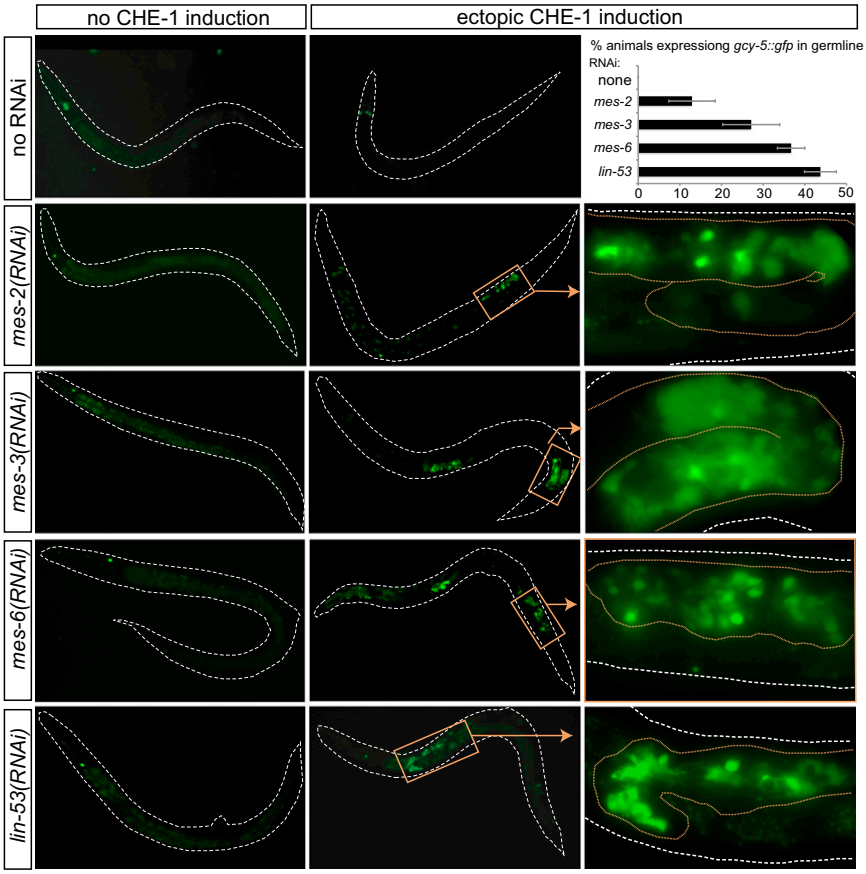

Figure 1. Knockdown of Members of the PRC2 Complex Allow *che-1*-Mediated Conversion of Germ Cells to Neurons

Larval progeny of RNAi-treated animals were analyzed for *gcy-5::gfp* (ASE fate marker; *ntIs1* transgene) expression ~24 hr after heat-shock induction of *che-1* (*otIs305* transgene). Right panels show blowups of boxed regions in middle panels, with germlines outlined by brown stippled lines. The top-right panel shows penetrance of conversion phenotypes after *che-1* induction at the ~L4 stage (at least three independent experiments, n = 90–300 for each RNAi). Error bars for each data set represent the SEM. The incomplete penetrance is most likely due to the incomplete effect of RNAi (as quantified in Figure S1). We show with antibody staining that the germline conversion phenotype cannot be explained by improved germline expression of *che-1* from the heat-shock vector (Figure S2). See also Experimental Procedures for more comments on transgene expression in the germline.

See also Figures S1, S2, S4, S5, and S6.

et al., 2011), did not reveal any obvious *lin-53*-like phenotypes for individual members of the many complexes with which the LIN-53/Rbbp4,7 protein is known to associate. As a result, the mechanism by which LIN-53 operates to prevent a germ-cell-to-neuron conversion remained an open question. However, negative results from this screen were difficult to interpret, mainly because RNAi of many of the various LIN-53 complex components resulted in infertility or early developmental defects, thereby precluding analysis of the germline.

We focused our analysis on the well-characterized Polycomb repressive complex 2 (PRC2), which in vertebrates and *Drosophila* contains the LIN-53 orthologs Rbbp4,7 (CAF1 in *Drosophila*), the H3K27 methyltransferase Ezh2 (Enhancer of Zeste in *Drosophila*), the WD40 protein Eed (Extra sex combs in *Drosophila*), and other associated proteins (Kuzmichev et al., 2002; Margueron and Reinberg, 2011). Similarly, in *C. elegans*, the PRC2 complex has been shown to contain the H3K27 methyltransferase MES-2/Ezh2 and two accessory proteins, MES-3 and the WD40 protein MES-6/Eed (Bender et al., 2004; Xu et al., 2001). Ectopic CHE-1 expression in *mes-2* and *mes-3* null mutants that lack both maternal and zygotic gene activity did not induce neurons in the germline (data not shown), but this is because the germline of such animals degenerates during larval stages (Capowski et al., 1991). In contrast, partial knockdown of *mes-2*, *mes-3*, and *mes-6* by RNAi in a genetic background that was not sensitized for RNAi improved the fertility and viability of double-stranded RNA (dsRNA)-treated animals, allowing the production of more germ cells, and these germ cells appeared superficially normal (Figure S1). After feeding animals with dsRNA against *mes-2*, *mes-3*, and *mes-6*, we induced *che-1* expression in the progeny of dsRNA-fed animals in all tissues through the heat-shock promoter, at approximately mid-larval stages. Feeding of control dsRNA or no dsRNA resulted in heat-shock-induced *che-1* being able to ectopically induce the ASE fate marker *gcy-5* exclusively in a small number of head neurons. In contrast, RNAi of each member of the *C. elegans* PRC2 complex (*mes-2/Ezh2; mes-3* and *mes-6/Eed*) resulted in $che\text{-}1^{heat\text{-}shock}$ -dependent *gcy-5* expression in the germline (Figure 1), providing the first hint that, as in *lin-53(RNAi)* animals, the germ cells may have converted into ASE-like neurons. This effect is not merely the result of improved germline expression of *che-1*, as shown by antibody staining (Figure S2). Neuron-like conversion is not observed in zygotic *mes* null mutant animals that still have a maternal *mes* gene contribution (M+Z−), suggesting that partial (but not complete) elimination of maternal *mes* by RNAi allows germ cell survival and generates susceptibility to conversion.

To study the cell-fate conversion in more detail, we performed RNAi against *mes-2*, *mes-3*, and *mes-6*, and induced *che-1* in a number of transgenic animals that express several reporter gene constructs. These included a second marker of ASE fate (*ceh-36*) and two panneuronal markers (*unc-33* and *snb-1*). We found that all of these markers were induced in the germline under these circumstances (Figure 2A). Neuronal marker induction was not only observed at the level of reporter transgenes but was also confirmed by single-molecule fluorescence in situ hybridization (smFISH; Raj et al., 2008), which revealed induction of endogenous neuronal genes, normally expressed

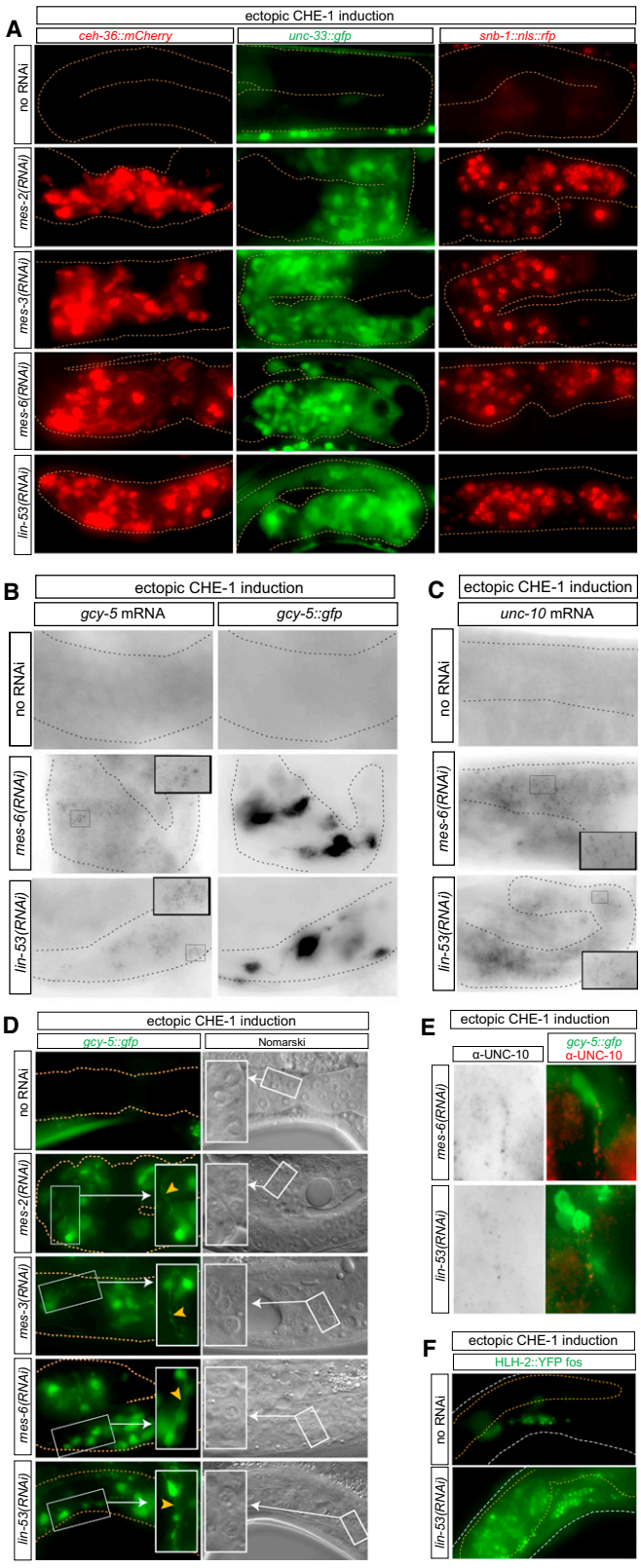

Figure 2. Detailed Characterization of Germ-Cell-to-Neuron Conversion

(A) The progeny of RNAi-treated animals were analyzed for the expression of several additional markers (*ceh-36*: *otIs264; unc-33: otIs118; snb-1: otEx4445*) after ~24 hr of heat-shock promoter-mediated *che-1* induction at larval stages (*otIs305* transgene). The penetrance of this phenotype ranged from 20% to 50% for the various markers (n = 30–60 for each marker, for each RNAi).

(B and C) smFISH shows induction of endogenous genes in converted germ cells. *gcy-5* (B) and *unc-10* (C) are induced in the germline of animals in which either *lin-53* or the representative PRC2 complex component *mes-6* was knocked down by RNAi, and in which *che-1* expression was ectopically induced. Individual mRNA molecules show up as individual black dots. In (B), the *gcy-5::gfp* transgene (which only contains the *gcy-5* promoter and will therefore not be picked up by the smFISH probes) expression pattern shows extensive overlap with endogenous mRNA expression.

(D) Germ cells acquire a neuron-like morphology in terms of nuclear morphology (from "fried-egg" germ cell nuclei to speckled neuronal cell nuclei; right panels, including blowup in white box) and axo/dendritic extensions (arrowheads; left panels, including blowup in white box).

(E) Converted germ cells express the presynaptic protein UNC-10/Rim, which clusters along the length of a neuronal extension (arrowheads). Left and right panels show the same image.

(F) Induction of the immature neuronal marker *hlh-2*, as assessed using a fosmid reporter transgene (*otEx4720*).

See also Figures S2, S3, S4, S5, and S6.

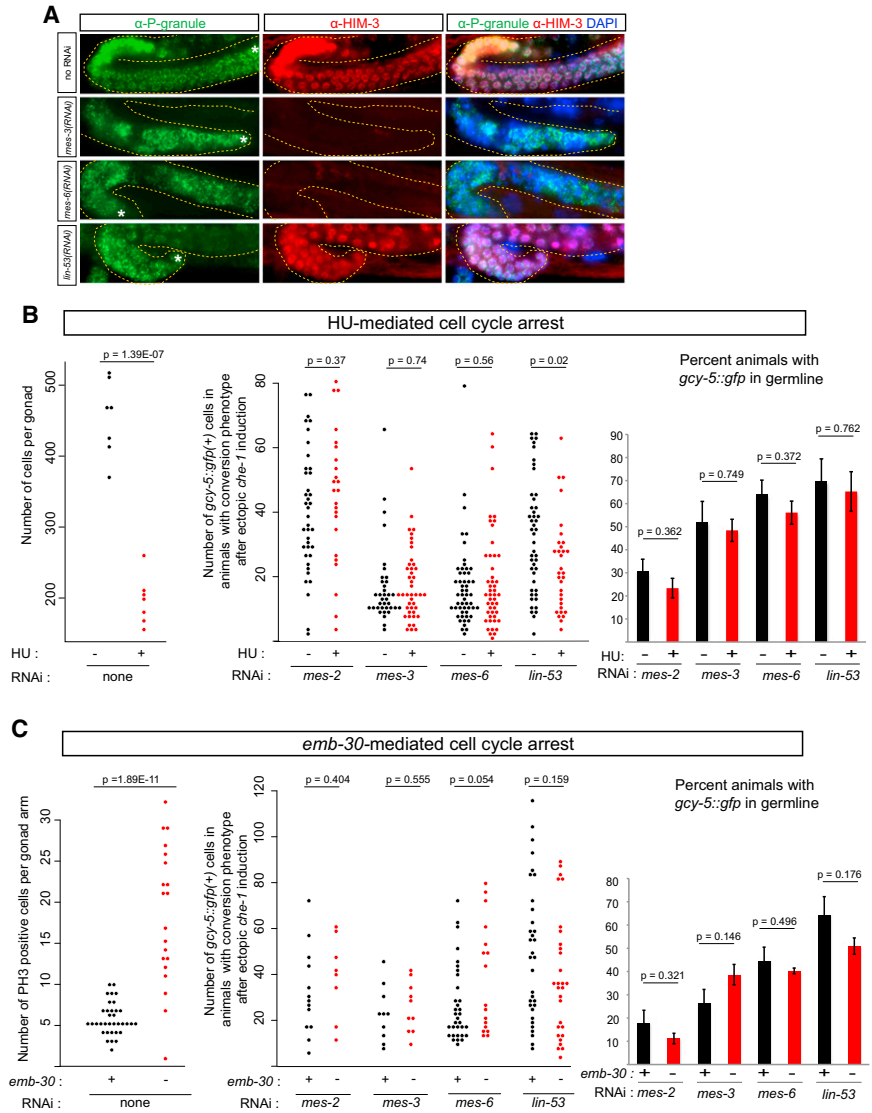

Figure 3. Mitotic Germ Cells Are Converted but Mitosis Is Not Required

(A) RNAi knockdown of *mes* genes inhibits entry into meiosis, as assessed by staining with the meiotic marker HIM-3. Knockdown of *lin-53* does not completely abolish entry into meiosis. Germ cells were still present in all cases, as assessed by staining with a P-granule specific antibody (OIC1D4). In the case of *mes-3(RNAi)* and *mes-6(RNAi)*, 80%–90% of animals that stained positive for OIC1D4 did not contain HIM-3-positive cells. The remaining 10%–20% animals that expressed HIM-3 had healthier-appearing gonads, indicating that RNAi knockdown was inefficient in these worms. More than 90% of *lin-53(RNAi)* animals that stained positive for OIC1D4 also expressed HIM-3. Asterisks indicate the distalmost part of the gonad in the image.

(B) Cell-cycle arrest by HU treatment. Left panel: There are half as many germ cells in the gonads of HU-treated animals. Middle panel: The expressivity of germline conversion remained unchanged after HU-mediated cell-cycle arrest (−, no HU treatment; +, 5 hr HU treatment; see Experimental Procedures). Each dot represents an individual animal. The effectiveness of HU treatment was also assessed by the lack of EdU staining (Figure S7). Right panel: The penetrance (i.e., the number of animals displaying the phenotype) of conversion is also not significantly altered. Error bars for each data set represent the SEM.

(C) Cell-cycle arrest by shifting *emb-30(tn377ts)* mutants to the nonpermissive temperature. Left panel: On average, there were ~3 times more germ cells in metaphase after an 8 hr temperature shift. Middle panel: The expressivity of germline conversion upon ectopic *che-1* induction remained unchanged after *emb-30*-mediated cell-cycle arrest. Each dot represents an individual animal (scored ~24 hr after *che-1* induction at the L4 stage). Right panel: The penetrance (i.e., number of animals displaying phenotype) of conversion is also not significantly altered. Error bars for each data set represent the SEM.

See also Figures S2, S4, S5, S6, and S7.

in ASE (*gcy-5* and *unc-10*), in converted germ cells (Figures 2B and 2C). Moreover, germ cell nuclei lost their characteristic "fried-egg" morphology and acquired a speckled nuclear morphology characteristic of neurons, and there was a concomitant loss of expression of the germ cell marker PGL-1(Figure 2D; Figure S3). Most strikingly, marker-gene-expressing cells extended cellular axo-dendritic-like projections, demonstrating that germ cells do not merely derepress marker genes but are also morphologically transformed into neurons (Figure 2D). These extensions show clusters of presynaptic proteins, as

assessed by UNC-10/Rim antibody staining (Figure 2E), corroborating the neuronal nature of these converted cells. All of these *che-1*-dependent phenotypes in *mes-2*, *mes-3*, and *mes-6 (RNAi)* animals are highly similar to the phenotypes observed with *lin-53(RNAi)* (Figures 1 and 2; Tursun et al., 2011).

Focus of Action of the PRC2 Complex

mes-2/Ezh2 and *mes-6/Eed* are known to be broadly expressed in embryonic somatic cells and in embryonic and adult germ cells (Holdeman et al., 1998; Korf et al., 1998). To analyze *lin-53* expression, we generated a fosmid-based *lin-53* reporter in which *gfp* was inserted into the *lin-53* locus in the context of ~40 kb of genomic sequence, including the *lin-53* locus and several genes upstream and downstream of the locus. Transgenic animals expressing this reporter showed broad *lin-53::gfp* expression in all somatic tissues and the germline at all stages examined (Figures S4A and S4B). To test the most parsimonious model of PRC2 acting autonomously in the germ cells rather than in the surrounding somatic gonad to prevent *che-1*-induced germ-cell-to-neuron conversion, we sought to eliminate PRC2 specifically in germ cells by using animals that lack the RNA-directed RNA polymerase *rrf-1*. *rrf-1* is required for RNAi in many somatic cells (including the somatic gonad), but is not required for RNAi in the germline (Sijen et al., 2001). RNAi against *mes-2,3,6* and *lin-53* in an *rrf-1(pk1417)* mutant background will therefore eliminate gene function in germ cells but not in the somatic gonad. We found that in such animals, the *che-1*-induced conversion phenotype of *mes(RNAi) and lin-53(RNAi)* animals was still readily observable (Figures S4C and S4D).

Germ-Cell-to-Neuron Conversion Occurs in the Context of a Global Loss or Global Redistribution of H3K27 Trimethylation

Previous studies have shown that genetic removal of *mes-2*, *mes-3*, and *mes-6* results in a genome-wide loss of H3K27me3 in the germline that can be readily assessed by staining nuclei of *mes-2*, *mes-3*, or *mes-6* mutant cells with H3K27me3 antibodies (Bender et al., 2004). We found that RNAi knockdown of not only *mes-2*, *mes-3*, or *mes-6* but also *lin-53* caused a loss of H3K27me3 in germ cells (Figure S5). These results suggest that genome-wide removal of H3K27me3 correlates with the susceptibility of germ cells to be converted into neurons, and they further underscore the expected phenotypic similarity of *lin-53(RNAi)* and *mes-2/3/6(RNAi).*

Recent work has shown that PRC2-mediated H3K27 methylation is antagonized by H3K36 methylation, suggesting that H3K36me is at least partially responsible for the precise genome-wide distribution of H3K27me3 (Gaydos et al., 2012, this issue; Yuan et al., 2011). In *C. elegans*, the histone methyltransferase MES-4 is responsible for all H3K36me2 and contributes to H3K36me3 (Rechtsteiner et al., 2010). As shown in the accompanying article (Gaydos et al., 2012) and summarized in Figure S6, loss of *mes-4* causes a genome-wide redistribution of H3K27me3, resulting in a net decrease of H3K27me3 on many somatic genes, including ASE-expressed and panneuronal genes. We found that in *mes-4(RNAi)* animals, germ cells also become susceptible to *che-1*-induced neuron conversion (Figure S6). Taken together, our data indicate that disruption of H3K27 methylation patterns, either through genome-wide knockdown or through genomic redistribution, renders the genome accessible to regulatory inputs that drive specific somatic cellular fates.

Mitotic Cycling Is Not Required for CHE-1-Driven Germ-Cell-to-Neuron Conversion

Having established the importance of PRC2 in the germ-cell-to-neuron conversion process, we next asked whether PRC2(−) germ cells need to be in a specific cellular state to be converted into neuron types. In wild-type animals, germ cells are in various states of mitotic and ensuing meiotic maturation. We could rule out that being in a meiotic state is required for *che-1*-induced neuron conversion, because we found that RNAi against PRC2 components or *lin-53* prevents meiotic entry of germ cells, as deduced by a lack of staining of the meiotic marker HIM-3 (Figure 3A).

Cell division has been proposed to be an important mediator of transitions between different states of gene expression, and transcription-factor-induced cellular reprogramming is indeed aided by cells being mitotically active (Egli et al., 2008; Hanna et al., 2009). We therefore asked whether the susceptibility of *PRC2(RNAi)* mitotic germ cells to conversion requires the mitosis process per se. To address this question, we treated worms with dsRNA and arrested the cell cycle before inducing *che-1*$^{heat\text{-}shock}$, and then determined whether the arrested cells were still convertible. Cell-cycle arrest was achieved in two independent ways. First, we blocked the cell cycle chemically through hydroxyurea (HU) treatment. HU arrests the cell cycle in S phase, as previously documented in many defined settings, including the *C. elegans* germline (Fox et al., 2011). We confirmed the effect of HU by counting the reduction of germ cell number and by observing the loss of 5-ethynyl-2′-deoxyuridine (EdU) incorporation (Figures 3B and S7). We found that *PRC2(RNAi)* cells treated with HU could still be converted into ASE-like neurons through heat-shock induction of *che-1* (Figure 3B).

As an independent approach to investigate the role of the cell cycle, we blocked the cell cycle genetically with the use of a temperature-sensitive allele, *tn377*, of the cell-cycle regulator *emb-30*, an anaphase-promoting complex/cyclosome component (Furuta et al., 2000). We grew dsRNA-treated *emb-30(tn377ts)* animals at 15°C and inactivated *emb-30* by shifting the worms to 25°C 8 hr before *che-1* heat-shock induction. Through staining with PH3, a marker of metaphase, we confirmed that within these 8 hr, an increased number of germ cells indeed became mitotically arrested (Figure 3C). We found that ectopic *che-1* could still convert germ cells into neurons if PRC2 had been knocked down (Figure 3C). We conclude from these results that PRC2(−) cells can be directly reprogrammed into neurons without the need to pass through the cell cycle.

The Germ-Cell-to-Neuron Conversion Process Passes through an Immature Neuronal Stage

In our previous phenotypic characterization of converted neurons in the germline of *PRC2(RNAi)* animals after *che-1* expression, we focused on examining terminal markers of

ASE neurons but did not examine possible intermediary stages of the conversion process. Although many markers of immature neurons have been identified in vertebrates, the only broadly expressed, early neuronal marker in *C. elegans* of which we are aware is the bHLH cofactor *hlh-2*/Daughterless. *hlh-2* is expressed broadly in the developing nervous system during mid-embryogenesis, but its expression fades in postmitotic neurons (Krause et al., 1997). This is consistent with the activity of lineage-specific, proneural bHLH partners of *hlh-2*, which in most organisms studied to date (including *C. elegans*) operate transiently during development to ensure the induction of neuronal fate (e.g., Poole et al., 2011). *hlh-2* is not expressed in the germline of wild-type animals (with or without *che-1* induction) or in *PRC2(RNAi)* animals, but is transiently induced in the converted neurons of *PRC2(RNAi)*; *che-1(hs)* animals (Figure 2F).

Specificity of Somatic Fate Conversion

We next asked whether the removal of PRC2 components makes mitotic germ cells also susceptible to be driven to non-neuronal, somatic fates. To address this issue, we turned to the *C. elegans* MyoD homolog *hlh-1*, a factor that acts, in analogy to neuronal terminal selectors, as a direct regulator of terminal muscle features (Lei et al., 2010). Previously, we found that in *lin-53(RNAi)* animals, ectopic induction of *hlh-1* was not able to convert mitotic germ cells to muscle (Tursun et al., 2011). To probe this issue further, we generated new *hlh-1* transgenic lines that are less repetitive in nature than the ones previously used and therefore less prone to partial or complete silencing in the germline (Experimental Procedures and Figure S2). We found that upon knockdown of the PRC2 component *mes-6* or *lin-53*, *hlh-1* was indeed able to convert germ cells directly into muscle-like cells, as assessed by the induction of transgenic markers for two distinct muscle proteins, UNC-97/PINCH (a muscle dense body component that also localizes to muscle nuclei; Hobert et al., 1999), and muscle myosin (*myo-3*; Fire and Waterston, 1989) (Figures 4A and 4B). Moreover, using antibody staining (Figure 4C), we observed the induction of two additional muscle proteins: Kettin, a normal component of myofibrils (Ono et al., 2006), and the transcription factor UNC-120/SRF, which is one of the three components (along with HLH-1 and HND-1) of the muscle-specific regulatory signature (Fukushige et al., 2006). A morphological transformation was also observed in the form of converted cells displaying a distinctive muscle nuclear morphology, based on size and perinuclear localization of UNC-97 (Figure 4).

Conclusions

Based on the phenotypic similarities that resulted from the knockdown of *lin-53* and the *mes-2*, *mes-3*, and *mes-6* genes, as well as the physical association of fly and vertebrate orthologs of their protein products (Kuzmichev et al., 2002; Margueron and Reinberg, 2011), we conclude that the *lin-53* phenotype we previously reported is likely the result of the functional disruption of the PRC2 complex. The conserved enzymatic role of PRC2 is the deposition of H3K27 di- and trimethyl marks, which are associated with developmentally regulated gene repression. PRC2 has numerous intricate biological roles that vary depending on cellular and temporal developmental contexts (Margueron and Reinberg, 2011; Zhang et al., 2011). For example, in *C. elegans*, PRC2 has been shown to play a role in restricting the plasticity of somatic cells in the developing embryo (Yuzyuk et al., 2009). Our findings suggest that PRC2 defines a chromatin state in germ cells that protects the genome from aberrant regulatory inputs. Disruption of this chromatin state renders germ cells susceptible to direct, cell-cycle-independent conversion into differentiated somatic cell types. These findings provide a conceptual framework for understanding the cellular context dependency of transcription factors that may be dictated by protective chromatin states. Protective chromatin states may differ among different cell types because the loss of PRC2 only makes germ cells, and not other somatic cell types, susceptible to cellular conversion. Recent work in *Drosophila* illustrated that repressed chromatin has distinct molecular signatures (van Steensel, 2011), and these signatures may be used in a cell-type-specific manner.

Our findings can also be viewed from the perspective of the multistep process of development from a germ cell via a zygote to a differentiated somatic cell type. We show that this process can be dramatically short-cut through the manipulation of chromatin modification patterns and provision of terminal selector transcription factors. The deposition of chromatin marks to specific genomic regions and the choice of a specific terminal selector transcription factor can be viewed as the ultimate goal for cells to achieve during development to adopt their final identity.

EXPERIMENTAL PROCEDURES

Strains and Transgenes

The following strains and transgenes were used:

OH9846: *otIs305 [hsp16-2prom::che-1::2xFLAG; rol-6(d)]; ntIs1 [gcy-5::gfp; lin-15(+)]*
SS186: *mes-2(bn11) unc-4(e120)*/mnC1 *dpy-10(e128) unc-52(e444)*II
SS262: *mes-3(bn35) dpy-5(e61)* I; sDp2(I;f)
OH9209: *otIs264 [ceh-36::tagrfp]*
OH10596: *otEx4720 [hlh-2 ^{fosmid}::yfp; rol-6(d)]*
OH439: *otIs118 [unc-33::gfp]*
OH10003: *pha-1; otEx4445[snb-1::NLSrfp; pBX]*
DG627: *emb-30(tn377)*III
NL2096: *rrf-1(pk1417)*I
OH10993: *otEx4944 [lin-53^{fosmid}::gfp; rol-6(d)]*
OH10995: *otIs377 [myo-3::mCherry]*
OH10994: *otEx4945 [hsp16-2prom::hlh-1::2xFLAG; rol-6(d)]; mgIs25 [unc-97::gfp].*

Like the *che-1* heat-shock array *otIs305* (and other previously described *che-1* arrays; Tursun et al., 2011), the *hlh-1* heat-shock array *otEx4945* is a complex array, generated by coinjection of PvuII-digested, bacterial genomic DNA (~150 ng/μl); the *hlh-1* expression construct (0.5 ng/μl); and pRF4 (2 ng/μl). In contrast to simple arrays, such complex arrays are not normally silenced in the germline (Tursun et al., 2009; L. Cochella, B.T., and O.H., unpublished data). The previously used *hlh-1* transgene (Tursun et al., 2011) is a simple array (Fukushige and Krause, 2005). The *lin-53* fosmid reporter was generated with 10 ng/μl lin-53::gfp fosmid, 2 ng/μl pRF4, and 135 ng/μl PvuII-digested, bacterial genomic DNA. The *hlh-2* fosmid reporter was a kind gift from the Greenwald laboratory.

The *lin-53* fosmid reporter was generated by fosmid recombineering (Tursun et al., 2009), using fosmid WRM0634aA12. This transgene does not rescue the

Cell PRESS
Open ACCESS

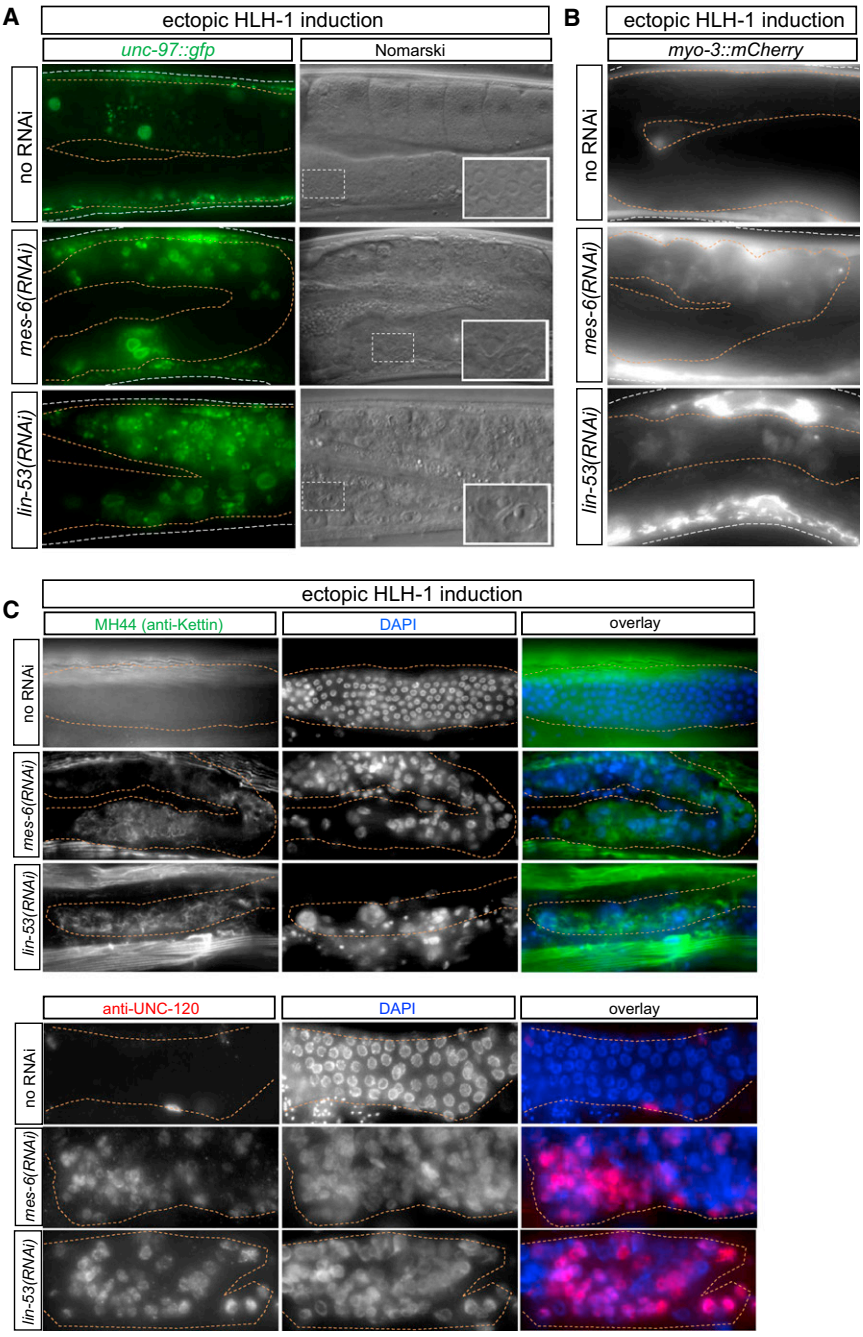

Figure 4. Conversion of Germ Cells into Muscle Cells

The progeny of RNAi-treated animals were analyzed for muscle marker expression ~24 hr after heat-shock promoter-mediated *hlh-1* induction at mid larval stages (*otEx4945* transgene).

(A) Induction of the LIM domain protein UNC-97, as observed with an *unc-97::gfp* translational fusion transgene *mgIs25*. UNC-97 protein is known to localize in muscle cells to both dense bodies (cellular attachment structures) and the nuclear periphery (Hobert et al., 1999). Some converted nuclei also showed a muscle-like morphology based on the size and localization of UNC-97 at the nuclear periphery.

(B) Induction of the myosin gene, as assessed with the *myo-3* transgene *otIs377*.

(C) Induction of the myofibrillar, actin-binding Kettin protein, as assessed with antibody MH44, and of the myogenic transcription factor UNC-120, as assessed by anti-UNC120 antibody staining.

See also Figures S2, S4, S5, and S6.

putative null (*n3368*). Primer sequences are available upon request. The resulting transgene, again generated as a complex array, is called *otEx4944*.

Antibody Staining, smFISH, and Microscopy

For antibody staining, we used a freeze-crack protocol on whole worms (Duerr, 2006). Worms were washed, suspended in 0.025% glutaraldehyde, and spread out between two frost-resistant glass slides. The slides were frozen on dry ice and cracked open to break the cuticle of the animals. Acetone/methanol fixation was used for most antibodies to prevent gonad extrusion. The freeze-cracked worms were incubated for 5 min each in ice-cold acetone and methanol. The worms were then washed off the slides in 1× PBS, blocked, and stained. Blocking was done in 1× PBS with 0.2% gelatin and 0.25% Triton for 30 min at room temperature. Antibodies were diluted in 1× PBS containing 0.1% gelatin and 0.25% Triton. Primary antibody was left on overnight at 4°C and secondary antibody was applied for 3 hr at room temperature. After the secondary antibody was washed off, the worms were incubated with DAPI for 15 min, washed again, and mounted on glass slides. The primary antibodies used were RIM2 (developed by Michael Nonet, obtained from the Developmental Studies Hybridoma Bank; used at 1:10 with 3.5% paraformaldehyde fixation); anti-PGL-1 (rabbit polyclonal antibody, 1:500, a gift from Susan Strome); P-granule component monoclonal antibody OIC1D4 (developed by Susan Strome, obtained from the Developmental Studies Hybridoma Bank, used at 1:5); anti-HIM-3 (1:500, a gift from Monique Zetka); Kettin MH44 antibody (obtained from Pamela Hoppe and used at 1:250; described in Francis and Waterston (1985); H3K27me3 (1:500; Millipore); anti-UNC-120 antibody (a gift from Michael Krause, used with 3.5% paraformaldehyde fixation at 1:10 dilution); anti-HA (1:50 with paraformaldehyde fixation; Roche); anti-FLAG (paraformaldehyde fixation; Sigma). All secondary antibodies were Alexa Fluor dyes used at 1:1,000 dilution.

smFISH was performed with the use of Custom Stellaris FISH probes purchased from Biosearch Technologies, and staining was done according to the manufacturer's protocol. μManager was used for image acquisition and processing (Edelstein et al., 2010).

RNAi

RNAi was done as previously described (Tursun et al., 2011). In brief, transgenic worms expressing heat-shock-inducible *che-1* or *hlh-1* in either the N2 wild-type background or mutant backgrounds (*emb-30* or *rrf-1*) were transferred to plates that were seeded with bacteria containing specific RNAi clones against *lin-53*, *mes-2*, *mes-3*, or *mes-6* at the L4 stage. Compared with *mes* null mutant animals, whose germline degenerates, the F1 progeny of RNAi-treated animals contained more germ cells, and these germ cells

appeared superficially normal as assessed by staining with germ cell markers (Figure S6, and shown as controls in Figures 2C and 3A). These worms were heat shocked at the L3–young-adult stage by incubation at 37°C for 30 min. The heat-shocked worms were kept at 25°C overnight and scored the following day. *emb-30* mutants were grown at 15°C, shifted to 25°C for 8 hr when F1 progeny on RNAi plates were at the L3–young-adult stage, heat shocked at 37°C, kept overnight at 25°C, and scored the next day.

Cell-Cycle Arrest by HU Treatment

HU treatment was performed as described previously (Fox et al., 2011). In brief, plates were seeded with MG1693 bacteria that had incorporated 5-ethynyl-2′-deoxyuridine (EdU). To assess cell-cycle arrest, HU at a final concentration of 250 μM was added to some of the plates. L4 animals, grown on OP50, were moved to the HU-treated and -untreated EdU-labeled bacteria plates. After 5 hr, these animals were washed off, freeze cracked on poly-L-lysine-coated slides, fixed with 3% paraformaldehyde, and stained with DAPI. The EdU detection reaction, which labels EdU with an Alexa-Fluor dye, was performed with the use of an EdU labeling kit (Invitrogen).

SUPPLEMENTAL INFORMATION

Supplemental Information includes seven figures and can be found with this article online at http://dx.doi.org/10.1016/j.celrep.2012.09.020.

LICENSING INFORMATION

ACKNOWLEDGMENTS

We thank Tim Schedl, Susan Strome, and Iva Greenwald for comments on the manuscript; Tim Schedl and members of his laboratory for technical advice; Monique Zetka, Susan Strome, Pamela Hoppe, Iva Greenwald, and Michael Krause for reagents; and Qi Chen for expert assistance in strain generation. This study was supported by the National Institutes of Health (1R21NS076191-01) and the Leona M. and Harry B. Helmsley Charitable Trust. T.P. was funded by a National Science Foundation predoctoral fellowship, and B.T. was funded by a Francis Goelet Postdoctoral Fellowship. O.H. is an Investigator of the Howard Hughes Medical Institute.

Received: May 21, 2012
Revised: July 18, 2012
Accepted: September 14, 2012
Published: October 25, 2012

REFERENCES

Bender, L.B., Cao, R., Zhang, Y., and Strome, S. (2004). The MES-2/MES-3/MES-6 complex and regulation of histone H3 methylation in *C. elegans*. Curr. Biol. *14*, 1639–1643.

Capowski, E.E., Martin, P., Garvin, C., and Strome, S. (1991). Identification of grandchildless loci whose products are required for normal germ-line development in the nematode *Caenorhabditis elegans*. Genetics *129*, 1061–1072.

Chang, S., Johnston, R.J., Jr., and Hobert, O. (2003). A transcriptional regulatory cascade that controls left/right asymmetry in chemosensory neurons of *C. elegans*. Genes Dev. *17*, 2123–2137.

Duerr, J.S. (2006). Immunohistochemistry. WormBook *19*, 1–61.

Edelstein, A., Amodaj, N., Hoover, K., Vale, R., and Stuurman, N. (2010). Computer control of microscopes using microManager. Curr. Protoc. Mol. Biol. *Chapter 14*, Unit14.20.

Egli, D., Birkhoff, G., and Eggan, K. (2008). Mediators of reprogramming: transcription factors and transitions through mitosis. Nat. Rev. Mol. Cell Biol. *9*, 505–516.

Etchberger, J.F., Lorch, A., Sleumer, M.C., Zapf, R., Jones, S.J., Marra, M.A., Holt, R.A., et al. (2007). The molecular signature and *cis*-regulatory architecture of a *C. elegans* gustatory neuron. Genes Dev. *21*, 1653–1674.

Fire, A., and Waterston, R.H. (1989). Proper expression of myosin genes in transgenic nematodes. EMBO J. *8*, 3419–3428.

Fox, P.M., Vought, V.E., Hanazawa, M., Lee, M.H., Maine, E.M., and Schedl, T. (2011). Cyclin E and CDK-2 regulate proliferative cell fate and cell cycle progression in the *C. elegans* germline. Development *138*, 2223–2234.

Francis, G.R., and Waterston, R.H. (1985). Muscle organization in *Caenorhabditis elegans*: localization of proteins implicated in thin filament attachment and I-band organization. J. Cell. Biol. *101*, 1532–1549.

Fukushige, T., and Krause, M. (2005). The myogenic potency of HLH-1 reveals wide-spread developmental plasticity in early *C. elegans* embryos. Development *132*, 1795–1805.

Fukushige, T., Brodigan, T.M., Schriefer, L.A., Waterston, R.H., and Krause, M. (2006). Defining the transcriptional redundancy of early bodywall muscle development in *C. elegans*: evidence for a unified theory of animal muscle development. Genes Dev. *20*, 3395–3406.

Furuta, T., Tuck, S., Kirchner, J., Koch, B., Auty, R., Kitagawa, R., Rose, A.M., and Greenstein, D. (2000). EMB-30: an APC4 homologue required for metaphase-to-anaphase transitions during meiosis and mitosis in *Caenorhabditis elegans*. Mol. Biol. Cell *11*, 1401–1419.

Gaydos, L., Rechtsteiner, A., Egelhofer, T., Carroll, C., and Strome, S. (2012). Antagonism between MES-4 and Polycomb repressive complex 2 promotes appropriate gene expression in *C. elegans* germ cells. Cell Rep. Published online October 25, 2012. http://dx.doi.org/10.1016/j.celrep.2012.09.019.

Hanna, J., Saha, K., Pando, B., van Zon, J., Lengner, C.J., Creyghton, M.P., van Oudenaarden, A., and Jaenisch, R. (2009). Direct cell reprogramming is a stochastic process amenable to acceleration. Nature *462*, 595–601.

Harrison, M.M., Ceol, C.J., Lu, X., and Horvitz, H.R. (2006). Some *C. elegans* class B synthetic multivulva proteins encode a conserved LIN-35 Rb-containing complex distinct from a NuRD-like complex. Proc. Natl. Acad. Sci. USA *103*, 16782–16787.

Hobert, O., Moerman, D.G., Clark, K.A., Beckerle, M.C., and Ruvkun, G. (1999). A conserved LIM protein that affects muscular adherens junction integrity and mechanosensory function in *Caenorhabditis elegans*. J. Cell Biol. *144*, 45–57.

Holdeman, R., Nehrt, S., and Strome, S. (1998). MES-2, a maternal protein essential for viability of the germline in *Caenorhabditis elegans*, is homologous to a *Drosophila* Polycomb group protein. Development *125*, 2457–2467.

Korf, I., Fan, Y., and Strome, S. (1998). The Polycomb group in *Caenorhabditis elegans* and maternal control of germline development. Development *125*, 2469–2478.

Krause, M., Park, M., Zhang, J.M., Yuan, J., Harfe, B., Xu, S.Q., Greenwald, I., Cole, M., Paterson, B., and Fire, A. (1997). A *C. elegans* E/Daughterless bHLH protein marks neuronal but not striated muscle development. Development *124*, 2179–2189.

Kuzmichev, A., Nishioka, K., Erdjument-Bromage, H., Tempst, P., and Reinberg, D. (2002). Histone methyltransferase activity associated with a human multiprotein complex containing the Enhancer of Zeste protein. Genes Dev. *16*, 2893–2905.

Lei, H., Fukushige, T., Niu, W., Sarov, M., Reinke, V., and Krause, M. (2010). A widespread distribution of genomic CeMyoD binding sites revealed and cross validated by ChIP-Chip and ChIP-Seq techniques. PLoS ONE *5*, e15898.

Loyola, A., and Almouzni, G. (2004). Histone chaperones, a supporting role in the limelight. Biochim. Biophys. Acta *1677*, 3–11.

Margueron, R., and Reinberg, D. (2011). The Polycomb complex PRC2 and its mark in life. Nature *469*, 343–349.

Ono, K., Yu, R., Mohri, K., and Ono, S. (2006). *Caenorhabditis elegans* kettin, a large immunoglobulin-like repeat protein, binds to filamentous actin and

provides mechanical stability to the contractile apparatuses in body wall muscle. Mol. Biol. Cell *17*, 2722–2734.

Poole, R.J., Bashllari, E., Cochella, L., Flowers, E.B., and Hobert, O. (2011). A Genome-Wide RNAi Screen for Factors Involved in Neuronal Specification in *Caenorhabditis elegans*. PLoS Genet. *7*, e1002109.

Raj, A., van den Bogaard, P., Rifkin, S.A., van Oudenaarden, A., and Tyagi, S. (2008). Imaging individual mRNA molecules using multiple singly labeled probes. Nat. Methods *5*, 877–879.

Rechtsteiner, A., Ercan, S., Takasaki, T., Phippen, T.M., Egelhofer, T.A., Wang, W., Kimura, H., Lieb, J.D., and Strome, S. (2010). The histone H3K36 methyltransferase MES-4 acts epigenetically to transmit the memory of germline gene expression to progeny. PLoS Genet. *6*, 6.

Sijen, T., Fleenor, J., Simmer, F., Thijssen, K.L., Parrish, S., Timmons, L., Plasterk, R.H., and Fire, A. (2001). On the role of RNA amplification in dsRNA-triggered gene silencing. Cell *107*, 465–476.

Tursun, B., Cochella, L., Carrera, I., and Hobert, O. (2009). A toolkit and robust pipeline for the generation of fosmid-based reporter genes in *C. elegans*. PLoS ONE *4*, e4625.

Tursun, B., Patel, T., Kratsios, P., and Hobert, O. (2011). Direct conversion of *C. elegans* germ cells into specific neuron types. Science *331*, 304–308.

Uchida, O., Nakano, H., Koga, M., and Ohshima, Y. (2003). The *C. elegans* che-1 gene encodes a zinc finger transcription factor required for specification of the ASE chemosensory neurons. Development *130*, 1215–1224.

van Steensel, B. (2011). Chromatin: constructing the big picture. EMBO J. *30*, 1885–1895.

Xu, L., Fong, Y., and Strome, S. (2001). The *Caenorhabditis elegans* maternal-effect sterile proteins, MES-2, MES-3, and MES-6, are associated in a complex in embryos. Proc. Natl. Acad. Sci. USA *98*, 5061–5066.

Yuan, W., Xu, M., Huang, C., Liu, N., Chen, S., and Zhu, B. (2011). H3K36 methylation antagonizes PRC2-mediated H3K27 methylation. J. Biol. Chem. *286*, 7983–7989.

Yuzyuk, T., Fakhouri, T.H., Kiefer, J., and Mango, S.E. (2009). The Polycomb complex protein mes-2/E(z) promotes the transition from developmental plasticity to differentiation in *C. elegans* embryos. Dev. Cell *16*, 699–710.

Zhang, Z., Jones, A., Sun, C.W., Li, C., Chang, C.W., Joo, H.Y., Dai, Q., Mysliwiec, M.R., Wu, L.C., Guo, Y., et al. (2011). PRC2 complexes with JARID2, MTF2, and esPRC2p48 in ES cells to modulate ES cell pluripotency and somatic cell reprogramming. Stem Cells *29*, 229–240.

Zhou, Q., and Melton, D.A. (2008). Extreme makeover: converting one cell into another. Cell Stem Cell *3*, 382–388.

Cell PRESS
Open ACCESS

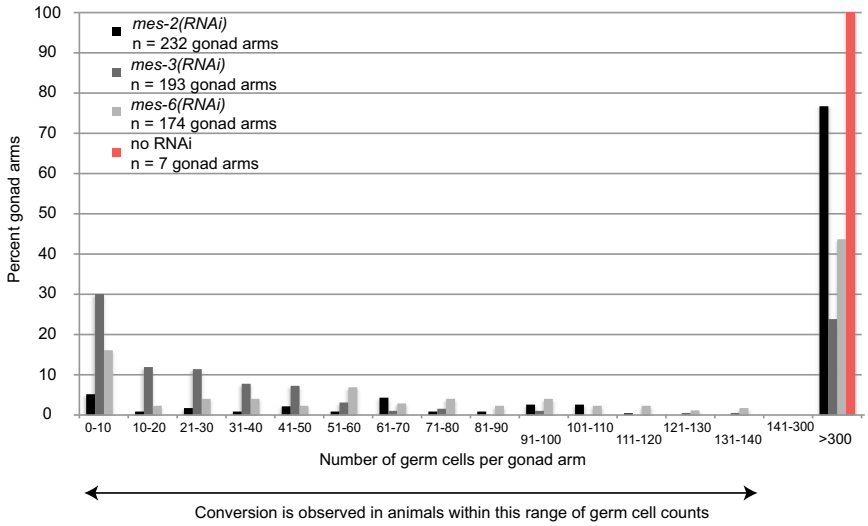

Figure S1. PRC2, RNAi, Reduces but Does Not Eliminate Germ Cells, Related to Figure 1

Quantification of the number of germ cells present in individual gonad arms of *mes-2*, *mes-3*, and *mes-6 (RNAi)* worms. *mes-2* and *mes-3* null mutants that lack a maternal load of protein usually contain <10 germ cells, while *mes-6* null mutants without a maternal protein load contain more germ cells (Capowski et al., 1991; Korf et al., 1998). In contrast, RNAi of *mes-2/3/6* results in variable phenotypes. Whereas some animals retain wild-type-like gonad arms (>300 germ cells per gonad arm), others show a severe reduction in germ cell numbers. The conversion phenotype is generally observed in gonad arms with 10–140 germ cells, suggesting that a sufficiently disrupted germline that still has some convertible germ cells remaining is required for cell-fate conversion. As shown in Figures 2C and 3A, the germ cells in *mes-2/3/6* animals still express the germ cell marker PGL-1 but do not progress into meiosis.

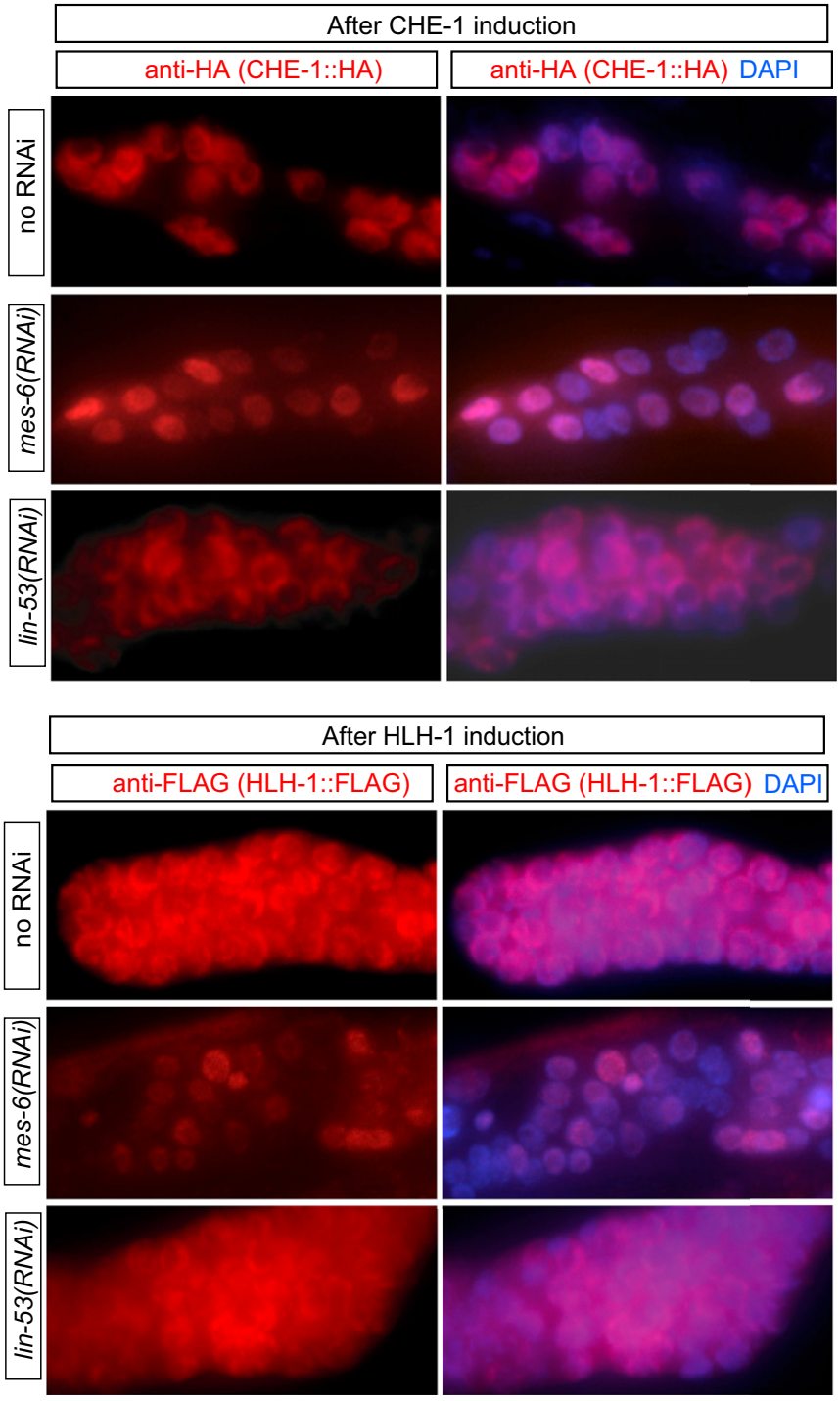

Figure S2. Transgene Expression in the Germline Before and After RNAi Treatment, Related to Figures 1, 2, 3, and 4

To test the possibility that the observed reprogramming of germ cells after knockdown of *lin-53* or PRC2 subunits (e.g., *mes-6*) can be attributed to increased expression levels of *che-1::HA* or *hlh-1::FLAG* due to transgene desilencing effects, we analyzed L3–L4 transgenic animals carrying *hsp::hlh-1::FLAG* (*otEx4945*) or *hsp::che-1::HA* (*otIs305*) by immunohistochemistry 4 hr after a 30 min heat-shock induction regimen at 37°C. Animals were either untreated or treated with RNAi against *lin-53* or *mes-6* and the F1 generation was immunostained. When we compared treated and untreated animals side by side, we found no obvious differences in staining; representative micrographs are shown here. Hence, *lin-53* or *mes-6* knockdown does not result in noticeably increased expression levels due to desilencing of transgenes. This is consistent with our observation that transgenes that are generated as complex arrays (e.g., the *che-1* and *hlh-1* arrays generated in this study through the use of low DNA concentrations for the expression plasmids mixed with complex DNA derived from PvuII digestion of bacterial genomic DNA) are not generally subject to transgene silencing (unpublished data).

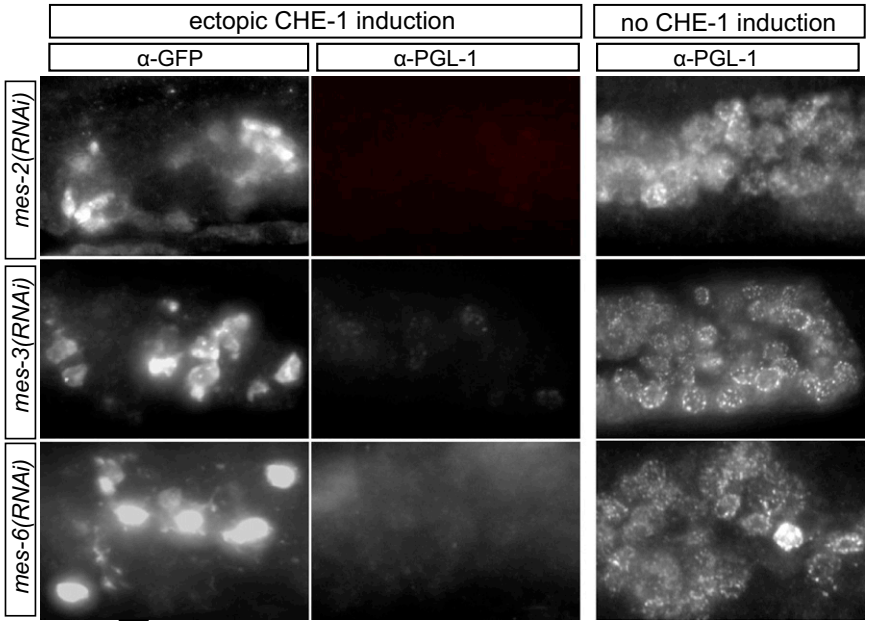

Figure S3. PGL-1 Expression in Converted Germ Cells, Related to Figure 2

Upon neuronal conversion, germ cells lose staining of the germ cell marker PGL-1. PGL-1 and *gcy-5::gfp* are mutually exclusive in >90% of converted gonads. In ~10% of converted gonads, faint PGL-1 is seen in some *gcy-5*-positive cells.

Cell PRESS
Open ACCESS

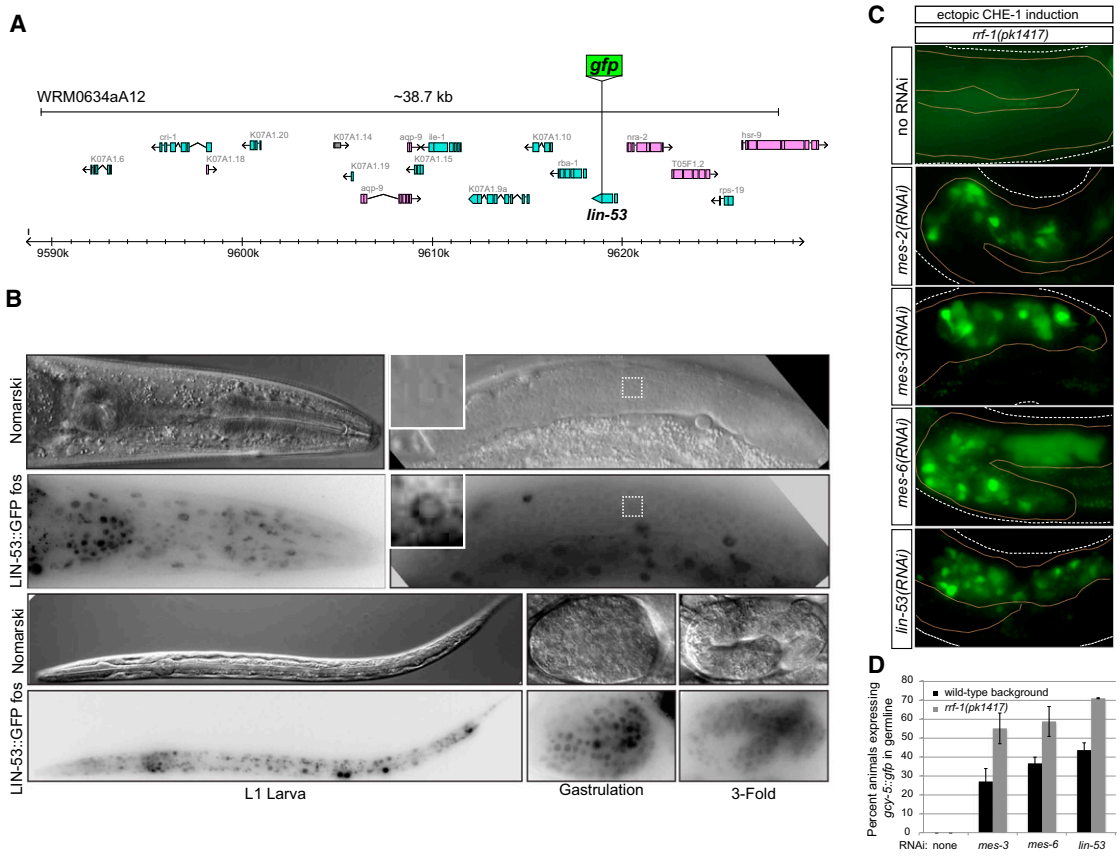

Figure S4. *lin-53* Expression Pattern and Focus of PRC2 Action in Germ Cells versus Somatic Gonads, Related to Figures 1, 2, 3, and 4

(A) The *lin-53* gene is contained within fosmid WRM0634aA12. *gfp* was recombineered in frame at the C terminus of *lin-53* according to Tursun et al. (2009).

(B) Expression pattern of LIN-53::GFP in array *otEx4944*. LIN-53::GFP is broadly expressed in all life stages and in many cells. Clockwise from top left: adult head; adult germline, faint LIN-53::GFP expression observed in germ cells (inset); 3-fold-stage embryo; mid-gastrulation-stage embryo; L1 larva. As is characteristic of extrachromosomal transgenes, expression is mosaic and variable in intensity.

(C) *rrf-1(pk1417)* mutants, which can carry out RNAi in the germline but not in the somatic gonad, also show the germline conversion phenotype in *mes(RNAi)* and *lin-53(RNAi)* animals ~24 hr after heat-shock induction of *che-1*. Stippled brown lines outline the gonads.

(D) Quantification of data in (C). The penetrance of the germline conversion phenotype is not diminished in *rrf-1(−/−)* animals compared with *rrf-1(+)* animals. In fact, *rrf-1* mutants show a slight increase in penetrance. Although this could be an artifact of RNAi experiments, it could also reflect the fact that the *rrf-1* mutants are generally healthier after RNAi knockdown of *mes-2/3/6* and *lin-53*.

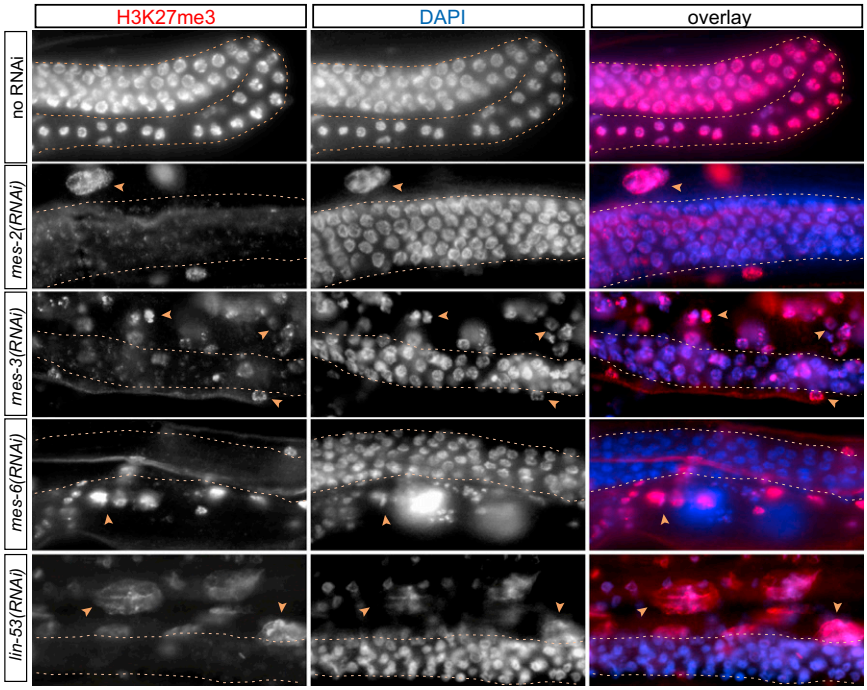

Figure S5. Depletion of PRC2 Results in Loss of H3K27me3 in the Germline, Related to Figures 1, 2, 3, and 4

RNAi knockdown of *mes-2*, *mes-3*, *mes-6*, and *lin-53* leads to a loss of global H3K27me3 in the germline (outlined), as assessed by staining for H3K27me3. Such a global loss is not obvious in the somatic cells (marked with arrowheads). Anti-H3K27me3 is shown in red and DAPI is shown in blue.

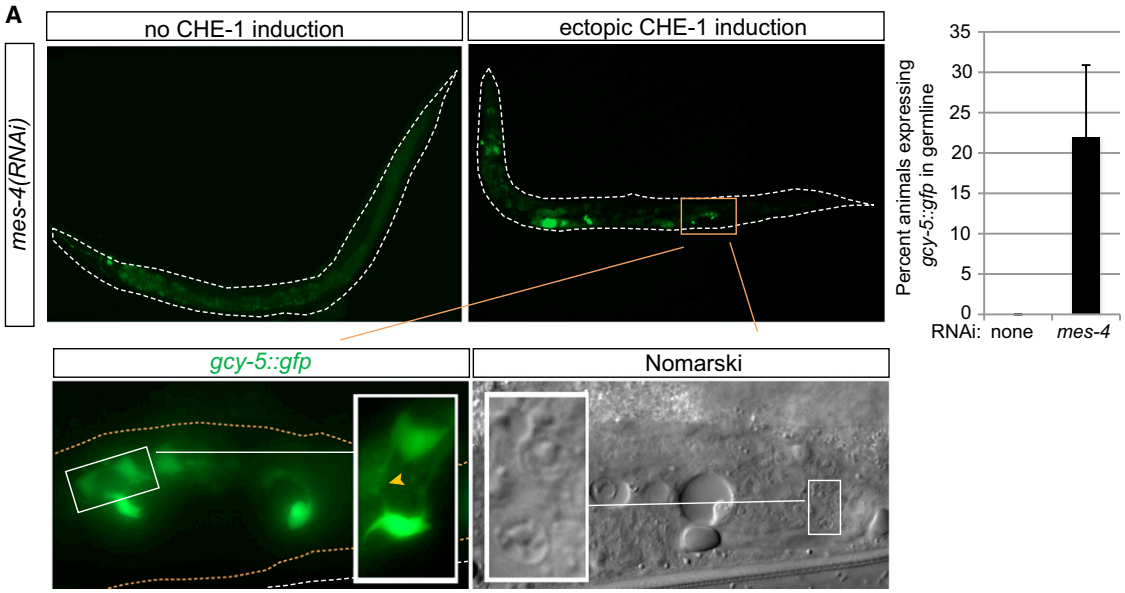

B

Histone Mods.	Gene Sets	wildtype	*PRC2(-)*	*mes-4(-)*
H3K27me3	ASE genes	++	-	+
	Other somatic genes	++	-	+
	Germline genes	-	-	+
H3K36me3	ASE genes	-	?	-
	Other somatic genes	-	?	-
	Germline genes	++	?	-

Figure S6. Germline Conversion in *mes-4(RNAi)*, Related to Figures 1, 2, 3, and 4

(A) Heat-shock induction of *che-1* in F1 progeny of *mes-4* dsRNA-treated animals results in a germ-cell-to-neuron conversion, as assessed by *gcy-5* expression, the presence of axo-dendritic projections (left panel and inset), and nuclear morphology (conversion of fried-egg-shaped germline to speckled neuronal nuclei, right panel and inset). RNAi alone, without *che-1* induction, does not result in conversion. The penetrance of this phenotype is shown in the bar graph (n = 159 from three individual experiments).

(B) Summary of chromatin marks in wild-type, *mes-4(–)*, and PRC2(–) animals. The relative level of each histone modification (H3K27me3 or H3K36me3) on different groups of genes is indicated schematically (++, high level; +, reduced level; –, absent). This summary is based on previously published data and the data of Gaydos et al. (2012) as follows: ChIP-chip experiments performed on early-embryo extracts to report on the state of chromatin inherited from the germline suggest that in wild-type embryos, *mes-4*-dependent H3K36me3 marks are enriched on germline-expressed genes (Rechtsteiner et al., 2010), whereas H3K27me3 marks are enriched on somatic genes, including a set of ASE-expressed genes (Gaydos et al., 2012; Etchberger et al., 2007). Mutation or knockdown of *mes-4* by RNAi results in a genome-wide depletion of H3K36me3 (Rechtsteiner et al., 2010). The accompanying article by Gaydos et al. (2012) shows that this H3K36me3 depletion also results in a redistribution of H3K27me3 marks such that in *mes-4(–)* embryos, there is a relative decrease of H3K27me3 on somatic genes and an increase on germline-expressed genes. There is also immunofluorescence evidence for antagonistic interactions between H3K27 methylation and H3K36 methylation in the germline (Bender et al., 2004). Therefore, we postulate that in our conversion experiments, both PRC2(RNAi) and *mes-4(RNAi)* allow for transcription-factor-dependent expression of somatic genes in germ cells because these germ cells now have decreased levels of H3K27me3 on somatic genes.

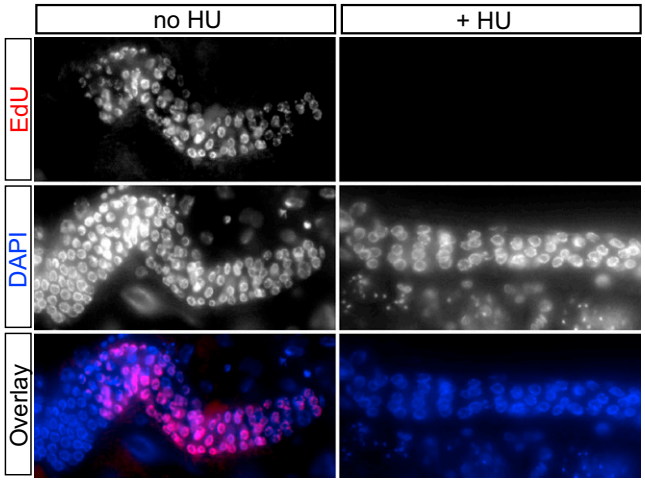

Figure S7. HU Treatment Arrests the Cell Cycle, Related to Figure 3

No EdU incorporation is seen in the germline after 5 hr of HU treatment. EdU is shown in red and DAPI is shown in blue. This test was done on a non-RNAi-treated, *hs::che-1*-containing transgenic strain (no *che-1* induction).